

Y3. A17

AEC

22/KAPL-2109 RESEARCH REPORTS

**KAPL-2109**

**AEC Research and Development Report**

**KNOLLS  
ATOMIC POWER  
LABORATORY**

UNIVERSITY OF  
ARIZONA LIBRARY  
Documents Collection  
MAR 13 1961

***Pressure and Thermal Stresses  
at a Pipe Attachment to a Sphere***

Operated for the  
United States Atomic  
Energy Commission by  
**GENERAL ELECTRIC**

***L. Deagle  
September 21, 1959***

metadc303895



UNCLASSIFIED

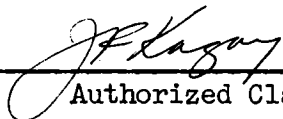
KAPL-2109

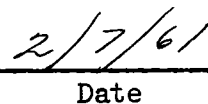
UC-34, Physics and Mathematics  
(TID-4500, 15th Edition)

PRESSURE AND THERMAL STRESSES AT  
A PIPE ATTACHMENT TO A SPHERE

L. Deagle

September 21, 1959

  
Authorized Classifier

  
Date

General Electric Company  
KNOLLS ATOMIC POWER LABORATORY  
Schenectady, New York  
Operated for the  
United States Atomic Energy Commission  
Contract No. W-31-109 Eng-52

UNCLASSIFIED

UNCLASSIFIED

LEGAL NOTICE

This report was prepared as an account of Government-sponsored work. Neither the United States, nor the Commission, nor any person acting on behalf of the Commission:

- A. Makes any warranty or representation, expressed or implied, with respect to the accuracy, completeness, or usefulness of the information contained in this report, or that the use of any information, apparatus, method, or process disclosed in this report may not infringe privately owned rights; or
- B. Assumes any liabilities with respect to the use of, or for damages resulting from the use of any information, apparatus, method, or process disclosed in this report.

As used in the above, "person acting on behalf of the Commission" includes any employee or contractor of the Commission, or employee of such contractor, to the extent that such employee or contractor of the Commission, or employee of such contractor prepares, disseminates, or provides access to, any information pursuant to his employment or contract with the Commission, or his employment with such contractor.

Printed in USA. Price .75 cents. Available from the Office of Technical Services, Department of Commerce, Washington 25, D. C.

UNCLASSIFIED

## UNCLASSIFIED

KAPL-2109

UC-34, Physics and Mathematics  
(TID-4500, 15th Edition)

<u>Internal Distribution</u>	<u>No. of Copies</u>
AEC, SNROO	1
Ahern, WT	1
Burke, MP	1
Cooper, WE	1
Deagle, L	12
Document Library	4
Doonan, AN	1
Fritz, RJ	1
Hofmann, CS	1
Kagay, JF	1
McCalley, RB	1
Miller, DR	1
Technical Publications/Shaw, JG	1
TIG/Schmidt, CJ	6
Younkins, TD	1
<u>External Distribution</u>	
Aberdeen Proving Ground	3
Aerojet-General Corporation	1
Aerojet-General, San Ramon (I00-880)	1
AFPR, Boeing, Seattle	1
AFPR, Lockheed, Marietta	3
Air Force Special Weapons Center	2
ANP Project Office, Convair, Fort Worth	2
Alco Products, Inc.	1
Allis-Chalmers Manufacturing Company	1
Argonne Cancer Research Hospital	1
Argonne National Laboratory	10
Army Ballistic Missile Agency	1
Army Chemical Center	4
Army Signal Research and Development Laboratory	1
Atomic Bomb Casualty Commission	1
AEC Scientific Representative, Japan	1
Atomic Energy Commission, Washington	3
Atomics International	3
Babcock and Wilcox Company (NY00-1940)	4
Battelle Memorial Institute	2

UNCLASSIFIED

## UNCLASSIFIED

<u>External Distribution (continued)</u>	<u>No. of Copies</u>
Brookhaven National Laboratory	4
Brush Beryllium Company	1
Bureau of Ships (Code 1500)	1
Bureau of Yards and Docks	1
Carnegie Institute of Technology	1
Chicago Operations Office	1
Chicago Patent Group	1
Columbia University (Havens)	1
Columbia University (S00-187)	1
Combustion Engineering, Inc.	2
Convair-General Dynamics Corporation, San Diego	1
Defence Research Member	5
Defense Atomic Support Agency, Washington	1
Department of the Army, G-2	2
duPont Company, Aiken	3
duPont Company, Wilmington	1
Edgerton, Germeshausen and Grier, Inc., Las Vegas	1
Frankford Arsenal	1
General Atomic Division	1
General Electric Company (ANPD)	2
General Electric Company, Richland	6
General Electric Company, St. Petersburg	1
General Nuclear Engineering Corporation	1
Gibbs and Cox, Inc.	1
Goodyear Atomic Corporation	2
Grand Junction Operations Office	1
Iowa State College	2
Jet Propulsion Laboratory	2
Los Alamos Scientific Laboratory	2
Lovelace Foundation	1
Maritime Administration	1
Martin Company	1
Midwestern Universities Research Association	2
Mound Laboratory	1
National Aeronautics and Space Administration, Cleveland	1
National Bureau of Standards	2
National Bureau of Standards (Library)	1
National Lead Company of Ohio	1
Naval Medical Research Institute	1
Naval Research Laboratory	3
New Brunswick Area Office	1
New York Operations Office	2

## UNCLASSIFIED

<u>External Distribution (continued)</u>	<u>No. of Copies</u>
New York University (Richtmyer)	1
Nuclear Development Corporation of America	2
Nuclear Metals, Inc.	1
Oak Ridge Institute of Nuclear Studies	1
Office of Naval Research	15
Office of Naval Research (Code 422)	1
Office of Ordnance Research	1
Office of Quartermaster General	1
Office of the Chief of Naval Operations	1
Ordnance Materials Research Office	1
Ordnance Tank-Automotive Command	1
Patent Branch, Washington	1
Pennsylvania State University (Blanchard)	1
Phillips Petroleum Company (NRTS)	4
Power Reactor Development Company	1
Pratt and Whitney Aircraft Division	3
Princeton University (White)	1
Public Health Service	2
Public Health Service, Savannah	1
Rensselaer Polytechnic Institute	1
Sandia Corporation, Albuquerque	1
Stevens Institute of Technology	1
Sylvania Electric Products, Inc.	1
Technical Research Group	1
Tennessee Valley Authority	1
Texas Nuclear Corporation	1
The Surgeon General	1
Union Carbide Nuclear Company (ORGDP)	2
Union Carbide Nuclear Company (ORNL)	5
Union Carbide Nuclear Company (Paducah Plant)	1
USAF Project RAND	1
U. S. Geological Survey, Denver	1
U. S. Geological Survey, Menlo Park	1
U. S. Geological Survey, Naval Gun Factory	1
U. S. Geological Survey, Washington	1
U. S. Naval Ordnance Laboratory	1
U. S. Naval Postgraduate School	1
U. S. Naval Radiological Defense Laboratory	2
U. S. Patent Office	1
University of California at Los Angeles	1
University of California, Berkeley	2
University of California, Livermore	4

UNCLASSIFIED

KAPL-2109

## UNCLASSIFIED

<u>External Distribution (continued)</u>	<u>No. of Copies</u>
University of California, San Francisco	1
University of Puerto Rico	1
University of Rochester	1
University of Rochester (Marshak)	2
University of Washington (Geballe)	2
University of Washington (Rohde)	1
Walter Reed Army Medical Center	1
Watertown Arsenal	1
Westinghouse Electric Corporation	4
Westinghouse Electric Corporation (Schafer)	2
Wright Air Development Center	6
Yale University (Breit)	1
Yale University (Schultz)	1
Yankee Atomic Electric Company	1
Technical Information Service Extension	325
Office of Technical Services, Washington	<u>75</u>
Total	646



CONTENTS

	<u>Page</u>
SYMBOLS . . . . .	ix
ABSTRACT . . . . .	xi
INTRODUCTION . . . . .	1
DISCUSSION . . . . .	1
APPLICATION OF THE NOMOGRAPHS TO A DESIGN PROBLEM . . . . .	4
COMPARISON WITH EXPERIMENTAL RESULTS . . . . .	7
SAMPLE PROBLEM . . . . .	8
CONCLUSIONS . . . . .	10
REFERENCES . . . . .	12
APPENDIX I . . . . .	A1
APPENDIX II . . . . .	A5

ILLUSTRATIONS

<u>No.</u>	<u>Title</u>	<u>Page</u>
1	Comparison of Measured Stresses with Calculated Stresses for Various External Fillet Radii (Models N-8F, N-8G, N-8H) (KS-40734). . . . .	2
2	Comparison of Measured Stresses with Calculated Stresses for Various External Fillet Radii (Models N-9A, N-9B, N-9C, N-9E) (KS-40735) . . . . .	3
3	Effective Increase in the Wall of the Cylinder Due to the Presence of the Fillet . . . . .	5
4	Bending Stress in the Cylinder at the Junction of a Cylinder and Sphere for a Difference in Average Wall Temperature (KS-26390) . . . . .	6
5	Hoop Stress in the Cylinder at the Junction of a Cylinder and a Sphere for a Difference in Average Wall Temperature (KS-26391). . . . .	6
6	Hoop Stress in the Sphere at the Junction of a Cylinder and a Sphere for a Difference in Average Wall Temperature (KS-26392). . . . .	7
7	Stress Notation . . . . .	8
A-1	Analytical Model with Internal Pressure . . . . .	A.1
A-2	Analytical Model with "Step" Temperature Change . . . . .	A.5
A-3	Bending Stress in the Cylinder (KS-26480) . . . . .	A.7
A-4	Hoop Stress in the Cylinder (KS-26481) . . . . .	A.8
A-5	Hoop Stress in the Sphere (KS-26482) . . . . .	A.9

## SYMBOLS

<u>Symbol</u>	<u>Definition</u>	<u>Unit</u>
a	= mean radius of cylinder	in.
$D_c$	$= \frac{Et_c^3}{12(1 - \nu^2)}$	in.-lb
$D_s$	$= \frac{Et_s^3}{12(1 - \nu^2)}$	in.-lb
E	= modulus of elasticity	psi
H	= radial shear on section in direction perpendicular to x	lb/in.
i	= subscript refers to internal stress	-
$K_B$	= stress concentration factor for a shouldered plate in bending	-
$K_t$	= stress concentration factor for a shouldered plate in tension	-
$M_x$	= axial bending moment per unit of circumference	in.-lb/in.
o	= subscript refers to external stress	-
p	= pressure acting normal to middle surface of the shell (positive when acting away from shell axis)	psi
R	= mean radius of sphere	in.
r	= external fillet radius between cylinder and sphere	in.
$t_c$	= cylinder wall thickness	in.
$t_s$	= sphere wall thickness	in.
W	= rotation, change of angle of tangent line to middle surface	rad
w	= radial displacement with respect to the center line of the cylinder	in.
x	= axial coordinate along the cylinder	in.
y	= circumferential coordinate in a plane normal to the axis of the cylinder	in.
$\alpha$	= coefficient of thermal expansion	1/°F

<u>Symbol</u>	<u>Definition</u>	<u>Unit</u>
$\beta_c^4$	$= \frac{3(1 - \nu^2)}{a^2 t_c^2}$	in. <sup>-4</sup>
$\beta_s^4$	$= \frac{3(1 - \nu^2)}{R^2 t_s^2}$	in. <sup>-4</sup>
$\Delta T$	= temperature difference between the cylinder and sphere (positive when the sphere is at a higher temperature than the cylinder)	°F
$\nu$	= Poisson's ratio = 0.3	-
$\sigma_{bc}$	= axial bending stress in the cylinder	psi
$\sigma_{bs}$	= meridional bending stress in the sphere	psi
$\sigma_n$	= stress in circumferential (hoop) direction on the outside surface of the cylinder or inside surface of the sphere*	psi
$\sigma_{nom}$	= $\frac{pR}{2t_s}$ in sphere; $\frac{pa}{t_c}$ in cylinder	psi
$\sigma_t$	= stress in the axial direction in the cylinder*	psi
$\sigma_{yc}$	= discontinuity hoop stress in cylinder	psi
$\sigma_{ys}$	= discontinuity hoop stress in sphere	psi
$\phi$	= angle between the normal to shell middle surface and shell axis in meridional plane	rad

---

\*Nominal stress plus discontinuity stress.

### ABSTRACT

Design nomographs and equations have been prepared for determining the bending stresses and hoop stresses at the junction of a cylinder and sphere when:

1. Internal pressure exists in the sphere and
2. There is a difference in average temperature between the cylinder and the sphere.

A correlation of calculated stresses and photoelastically determined stresses for models with internal pressure is presented.



## PRESSURE AND THERMAL STRESSES AT A PIPE ATTACHMENT TO A SPHERE

### INTRODUCTION

One of the simplest forms of nozzle connection for a pressure vessel is the planned intersection of a cylindrical pipe with a spherical cap on the vessel. When the vessel is subjected to internal pressure or when a difference in the average wall temperatures exists between the pipe and the vessel, an axisymmetric shear force and bending moment are required at the juncture of the pipe and the vessel to maintain continuity of the structure. These shear forces and bending moments produce bending stresses and hoop stresses in the two members which must be taken into consideration when the fatigue life of the structure is evaluated for cyclic loading conditions.

The bending moment and shear force at the juncture of the cylinder and sphere are statically indeterminate and must be evaluated by the use of the relative flexibilities of the cylinder and sphere. Expressions relating the deflection and rotation of the edge of the cylinder when axisymmetric shear forces and bending moments and uniform internal pressure are applied are given by S. Timoshenko.<sup>1</sup> To obtain similar expressions for the sphere, use is made of the approximate solution given by Timoshenko in which the sphere is replaced by a tangent cone at the edge of the opening. The solution developed for cylinders is then applied to this cone.

These expressions for the rotation and deflection of the cylinder and sphere are used to derive dimensionless formulas for the discontinuity bending stress and hoop stress on the outer surface of the cylinder, at its juncture with the sphere, and for the bending and hoop stress in the latitude plane on the inside surface of the sphere. Since the derived formulas are cumbersome, nomographs as well as curves have been prepared. They show discontinuity stresses for internal pressure and differential temperature loading for use in design calculations.

The total stress in the cylinder and sphere is obtained by adding the membrane stresses to the discontinuity stresses.

Formulas have been derived in the Appendix for the stresses in the cylinder and sphere with internal pressure and for a difference in average wall temperatures between the cylinder and the sphere.

### DISCUSSION

In this derivation of dimensionless formulas for the discontinuity stress and hoop stress, the principal assumptions are:

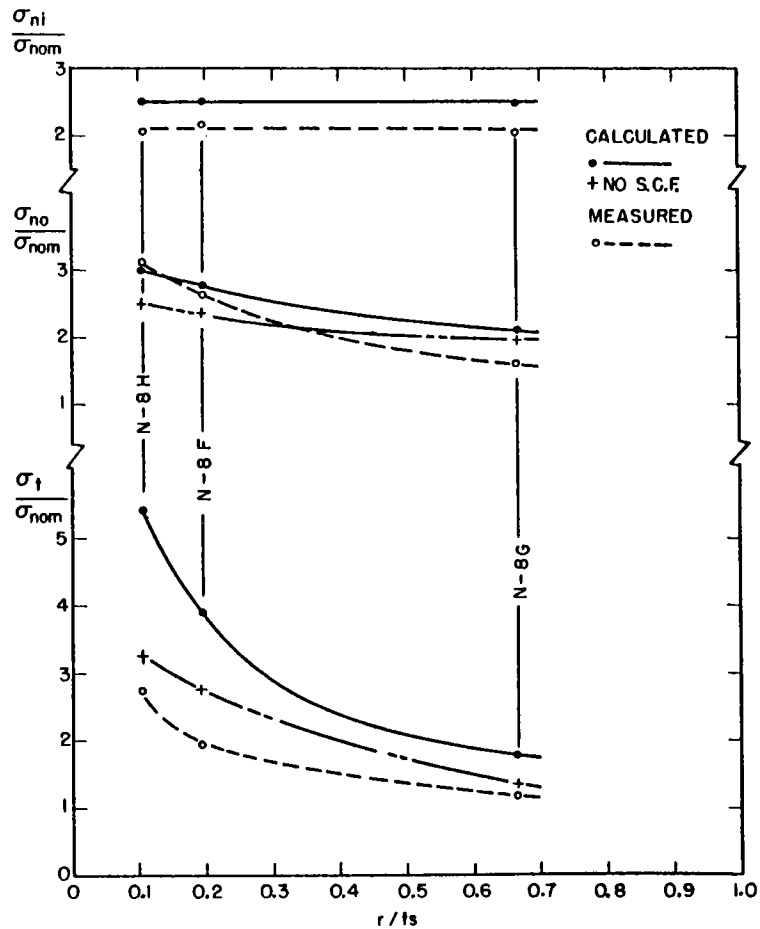


FIGURE 1. COMPARISON OF MEASURED STRESSES WITH CALCULATED STRESSES FOR VARIOUS EXTERNAL FILLET RADII (Models N-8F, N-8G, N-8H)

1. Thin-walled theory (wall thickness is small compared with the radius of the shell) is used.
2. The approximate solution for a cone tangent to the edge of the opening is used to describe the flexibilities of the sphere (see page 469 in Theory of Plates and Shells ).
3. The structure behaves elastically.
4. The modulus of elasticity is the same for the cylinder and the sphere.
5. Poisson's ratio = 0.3.

The analytical expressions are derived in terms of dimensionless ratios of wall thickness and radii, in order to minimize the number of variables. The discontinuity stresses in the cylinder are expressed as dimensionless ratios of the hoop membrane stress in the cylinder; the discontinuity stresses in the sphere are expressed as dimensionless ratios of the membrane stress in the sphere.



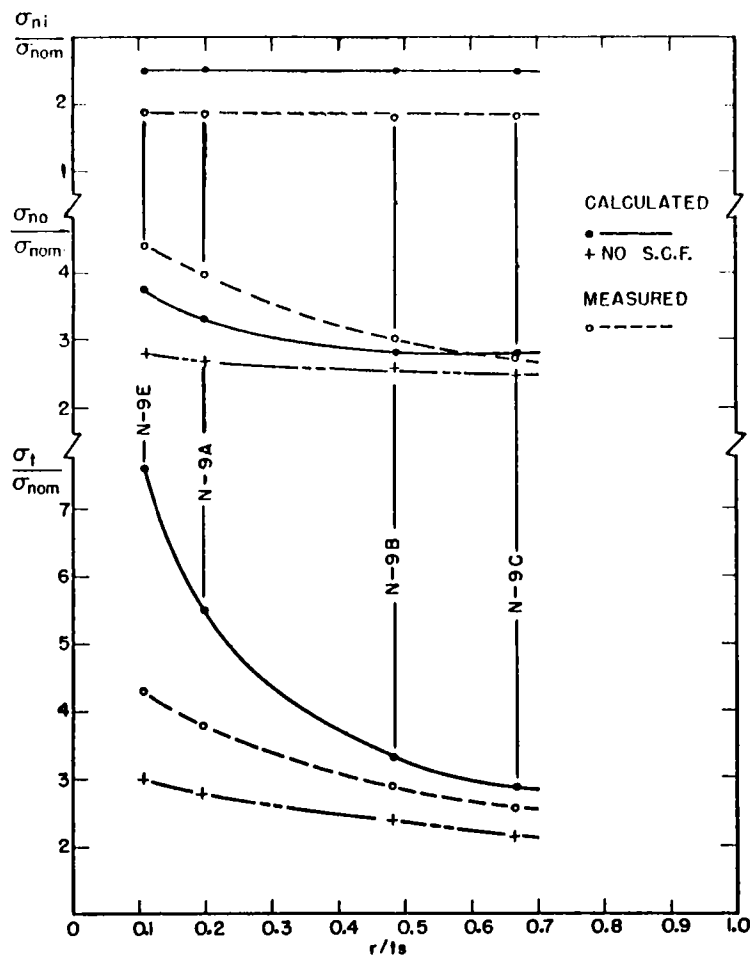


FIGURE 2. COMPARISON OF MEASURED STRESSES WITH CALCULATED STRESSES FOR VARIOUS EXTERNAL FILLET RADII (Models N-9A, N-9B, N-9C, N-9E)

Actual nozzle designs are not described exactly by the intersection of a cylinder and a sphere since nozzles usually have a fillet radius on the outside surface and a corner radius on the inside surface. The effects of various fillet radii and corner radii are shown in Figures 1 and 2. The dimensionless stress values given in these figures are for two groups of models in which the only variables are the inside and outside corner radii. On any given model these radii are equal. An approximate method for considering the effect of the outer fillet radius is given in the section on Application of the Nomographs to a Design Problem.

The approximations used for the influence coefficients of the sphere are expected to give the best estimate of the discontinuity stress when the ratio  $R/a$ , i.e., the included angle of the opening, is small. G. D. Galletly<sup>2</sup> recommends a more precise approximation for the influence coefficients when the included angle of the opening is less than  $\pi/6$ , e.g.,  $R/a > 3.86$ . However, in his examples, he shows that the simpler approximation that we use gives influence coefficients that are only

15% greater than those obtained by the more precise method when  $R/a \approx 5.5$ . The curves on Figures 1 and 2 are obtained for models having  $R/a$  equal to 7.45 and 2.5, respectively. These curves show that the effect of the outer fillet radius on stress concentration is a greater source of error than the approximations used in obtaining influence coefficients for the sphere. Therefore, we believe that Galletly,<sup>2</sup> for practical applications, sets too low a limit on the ratio for  $R/a$ . However, we do not know what the practical upper limits for this ratio should be.

The results obtained from the nomographs, prepared for design calculations, are accurate only to two places. If greater accuracy is desired, the analytical expressions can be used. However, in using a solution of this nature to predict the fatigue life of a real structure, we do not believe that more than two-place accuracy is justified.

Generally, in the design of pressure-retaining members, the minimum wall thickness for any given internal radii will be determined from the largest membrane stress. Therefore, the initial design of the structure for cyclic loading is based on these minimum values of wall thickness. If the design life predicted from the combination of membrane and discontinuity stresses for these minimum wall thicknesses is not satisfactory, the wall thickness of one or both members should be adjusted until a satisfactory life is achieved.

#### APPLICATION OF THE NOMOGRAPHS TO A DESIGN PROBLEM

The total stresses on the inside and outside of the cylinder and sphere are a combination of the discontinuity stresses obtained from the nomographs and the nominal stresses in the cylinder and sphere. An added correction is made in the form of a stress-concentration factor on the outside axial stress in the cylinder to account for the re-entrant angle between the cylinder and sphere.

To minimize the stress-concentrating effect of the re-entrant angle, a fillet forming a circular arc tangent to the cylinder and sphere is often used. The larger the fillet radius becomes, the closer the stress-concentration factor approaches unity. However, another effect takes place as the fillet radius becomes larger in proportion to the wall thickness of the cylinder. That is, the additional fillet material at the location of the maximum discontinuity moment acts to reduce the stress resulting from the axial force and the discontinuity moment. It does this without changing the magnitude of the moment since the stiffness of the cylinder or the sphere is not altered. The additional wall thickness to be attributed to the cylinder by the presence of the fillet is assumed to be equal to

$$r(1 - \cos 45^\circ) = 0.293r,$$

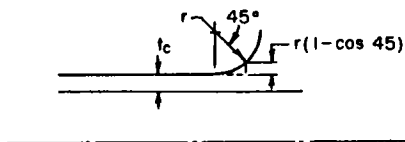


FIGURE 3. EFFECTIVE INCREASE IN THE WALL OF THE CYLINDER DUE TO THE PRESENCE OF THE FILLET

where  $r$  is the fillet radius as shown in Figure 3.

The formulas for computing the stresses in an actual design configuration are as follows:

For the cylinder, we obtain:

$$\frac{\sigma_t}{\sigma_{nom}} = K_B \times \frac{\sigma_{bc}}{\sigma_{nom}} \left( \frac{t_c}{t_c + 0.293r} \right)^2 + 0.5K_t \left( \frac{t_c}{t_c + 0.293r} \right) \quad (1)$$

and

$$\frac{\sigma_n}{\sigma_{nom}} = \frac{\sigma_{yc}}{\sigma_{nom}} + 1.0 + \frac{v\sigma_{bc}}{\sigma_{nom}} \left[ K_B \left( \frac{t_c}{t_c + 0.293r} \right)^2 - 1 \right], \quad (2)$$

where  $\sigma_{nom} = \frac{pa}{t_c}$

$K_B$  = the stress concentration factor (scf) for a shouldered plate in bending, expressed as a function of the fillet radius, and

$K_t$  = the scf for a shouldered plate in tension.

The values of these characteristics may be obtained from the literature.<sup>3,4,5</sup>

For the sphere, we obtain:

$$\frac{\sigma_n}{\sigma_{nom}} = \frac{\sigma_{ys}}{\sigma_{nom}} + 1.0, \quad (3)$$

where  $\sigma_{nom} = \frac{pR}{2t_s}$ .

The stresses in the cylinder are computed for the outer surface at the juncture with the sphere. The stress in the sphere is computed for the inside corner of the cylinder-sphere juncture.

The formulas for discontinuity stresses have been derived in the Appendix for internal pressure loading and for the limiting case of a "step" temperature change between the cylinder and the sphere. The discontinuity stresses for the step temperature change can be obtained from Figures 4 through 6.

In general, a temperature change occurs during operation at full pressure so that the total stress due to internal pressure and the temperature change is required for an evaluation of the fatigue strength of the nozzle joint. This combined stress can be obtained by combining

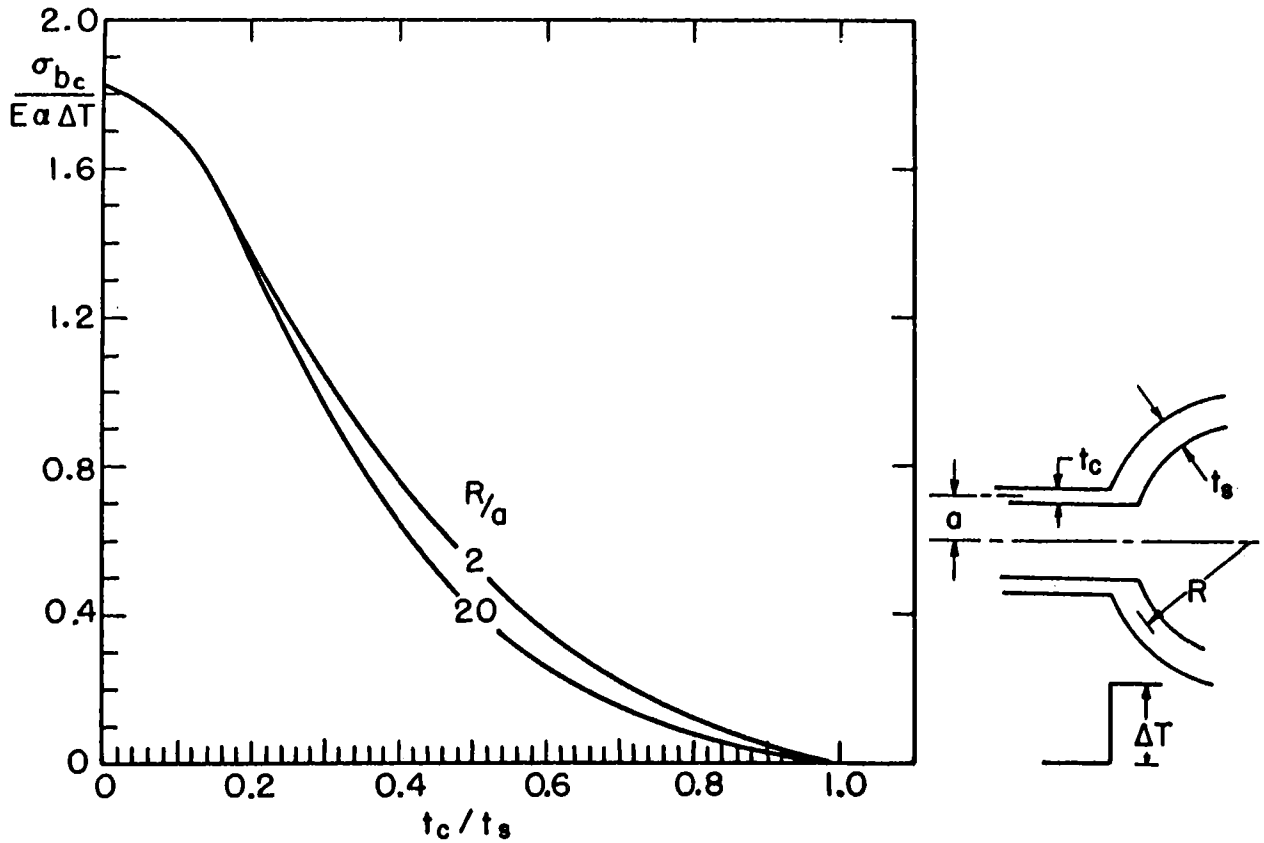


FIGURE 4. BENDING STRESS IN THE CYLINDER AT THE JUNCTURE OF THE CYLINDER AND SPHERE FOR A DIFFERENCE IN AVERAGE WALL TEMPERATURE

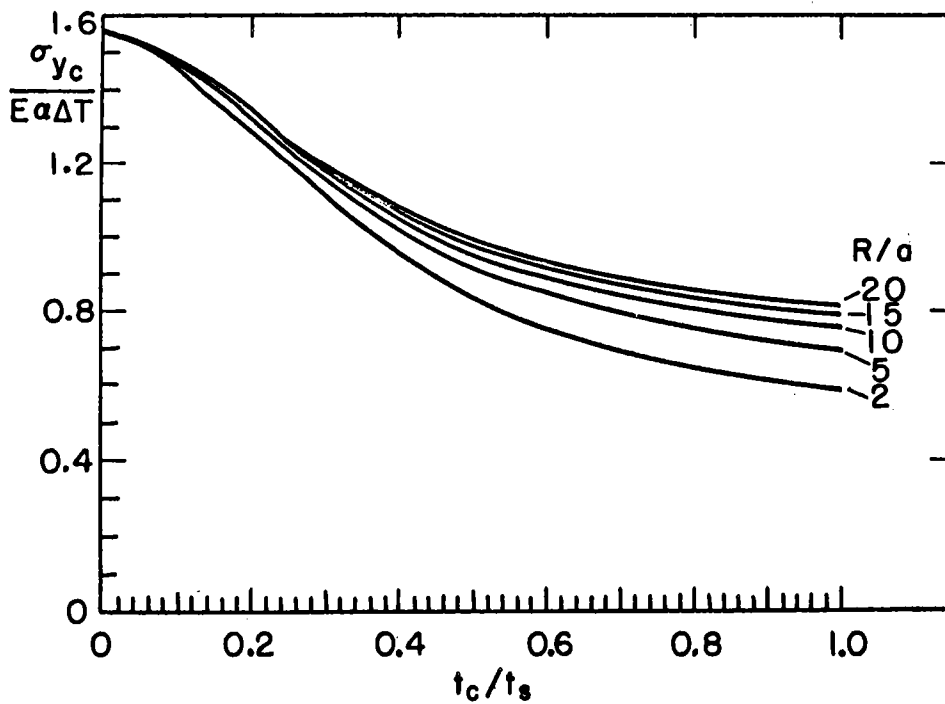


FIGURE 5. HOOP STRESS IN THE CYLINDER AT THE JUNCTURE OF A CYLINDER AND A SPHERE FOR A DIFFERENCE IN AVERAGE WALL TEMPERATURE

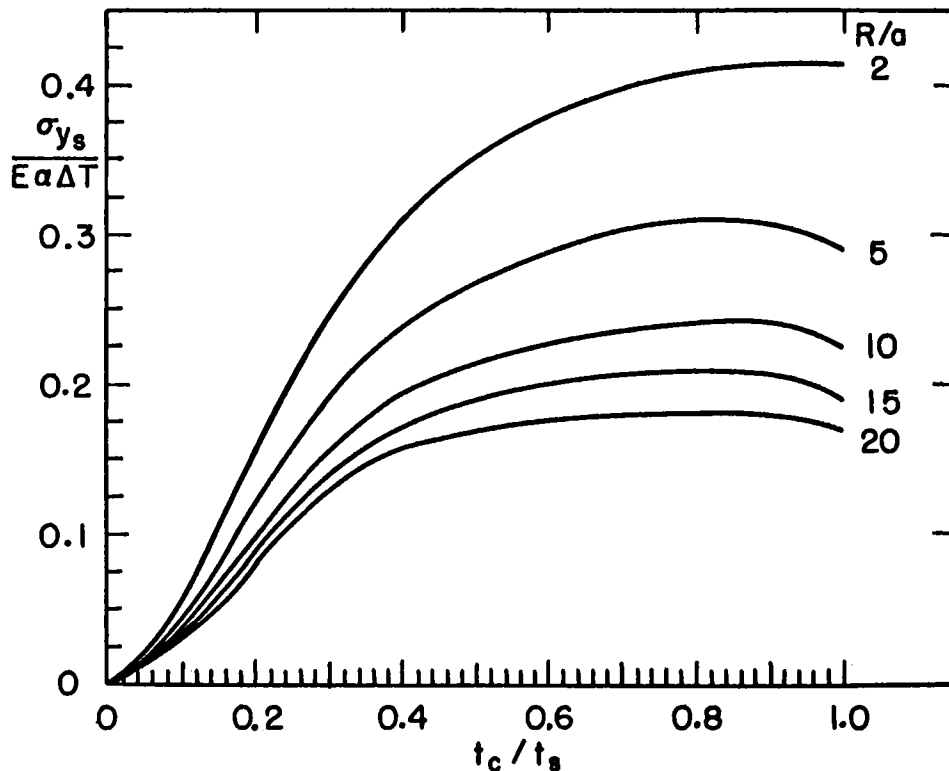


FIGURE 6. HOOP STRESS IN THE SPHERE AT THE JUNCTURE OF A CYLINDER AND A SPHERE FOR A DIFFERENCE IN AVERAGE WALL TEMPERATURE

algebraically the stresses resulting from the internal pressure with the stresses caused by the temperature change.

#### COMPARISON WITH EXPERIMENTAL RESULTS

Photoelastic tests have been made in a joint study conducted by the Bureau of Ships, the Atomic Energy Commission, and the Pressure Vessel Research Committee of the Welding Research Council. The results of this study are reported by Taylor et al.<sup>6,7,8</sup> Table 1 shows a comparison between the stresses determined from the charts and those obtained from the photoelastic investigation.

Dimensions of the models are taken from Table 2 of Taylor et al.;<sup>7</sup> they are given in Table 2.

The stress notation used in the photoelastic investigation is shown in Figure 7.

The test results shown in Figures 1 and 2 are taken from Taylor et al.<sup>8</sup> The dimensions of these models are given in Table 3.

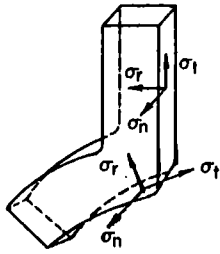


FIGURE 7. STRESS NOTATION

SAMPLE PROBLEM

To illustrate the use of the nomograms (Figures A.3 through A.5) and the calculation procedure, consider the determination of the stresses in Model N-5B, whose dimensions are given in Table 2. The

TABLE 1. COMPARISON BETWEEN CALCULATED AND MEASURED STRESSES

Model Number	Inside Values		Outside Values			
	$\sigma_n/\sigma_{nom}$		$\sigma_n/\sigma_{nom}$		$\sigma_t/\sigma_{nom}$	
	Measured	Calculated	Measured	Calculated	Measured	Calculated
N-1A	2.01	2.5	2.64	2.5	1.81	2.9
N-3D	1.71	2.1	1.90	2.0	1.76	2.2
N-1E	1.73	2.0	1.85	1.7	1.60	1.8
N-5B	2.27	2.6	2.73	2.3	1.60	1.8

NOTE:  $\sigma_{nom} = \frac{pR}{2t_s}$  in this table.

TABLE 2. DIMENSIONS OF MODELS

Model Number	Main Vessel, in.		Nozzle, in.		Corner	Fillet
	ID	Thickness	ID	Thickness	Radius, in.	Radius, in.
N-1A	14.333	0.600	2.875	0.250	0.333	0.333
N-3D	14.333	0.600	2.875	0.458	0.333	0.333
N-1E	14.333	0.600	2.875	0.600	0.333	0.333
N-5B	14.000	0.900	2.875	0.250	0.333	0.600

TABLE 3. DIMENSIONS OF MODELS

Model Number	Main Vessel, in.		Nozzle in.		Corner	Fillet
	ID	Thickness	ID	Thickness	Radius, in.	Radius, in.
N-8F	14.33	0.600	1.845	0.1605	0.118	0.118
N-8G	14.33	0.600	1.845	0.1605	0.40	0.40
N-8H	14.33	0.600	1.845	0.1605	0.063	0.063
N-9A	14.33	0.600	5.51	0.478	0.118	0.118
N-9B	14.33	0.600	5.51	0.478	0.289	0.289
N-9C	14.33	0.600	5.51	0.478	0.040	0.40
N-9E	14.33	0.600	5.51	0.478	0.063	0.063

ratios for use with Figures A.3, A.4, and A.5 are:

$$\frac{t_c}{t_s} = \frac{0.25}{0.9} = 0.278$$

$$\frac{R}{a} = \frac{7 + 0.45}{1.4375 + 0.125} = 4.77$$

$$\frac{R}{t_s} = \frac{7 + 0.45}{0.9} = 8.28 .$$

The discontinuity bending stress in the cylinder is obtained from Figure A.3 as follows:

1. Locate the point  $t_c/t_s = 0.278$  on the left-hand set of curves and from it draw a line vertically until the line intersects the curve at the point  $R/a = 4.77$  (interpolating between  $R/a = 4$  and  $R/a = 5$ ). With a horizontal line through this point, locate a point on the vertical axis B.
2. Draw a straight line between the point on axis B and  $R/t_s = 8.28$  on the diagonal scale to locate a point on scale T.
3. Locate point  $t_c/t_s = 0.278$  on the right-hand set of curves, and draw a line vertically until it intersects the curve  $R/a = 4.77$ . With a horizontal line through this point, locate a point on the vertical axis A.
4. Draw a straight line between the point on axis A and the point previously determined on scale T and read  $\frac{\sigma_{bc}}{\sigma_{nom}} = 2.1$ .

The discontinuity hoop stress in the cylinder is obtained from Figure A.4 and the discontinuity hoop in the sphere from Figure A.5 in the same manner as described for obtaining the bending stress. These values are, respectively,

$$\frac{\sigma_{yc}}{\sigma_{nom}} = 0.9$$

$$\frac{\sigma_{ys}}{\sigma_{nom}} = 1.6.$$

To obtain the values given in Table 1, the cylinder stresses are multiplied by  $\frac{2}{R/a \times t_c/t_s}$  to relate them to the nominal membrane stress in the sphere.

For the ratio of fillet radius to cylinder wall thickness, we obtain:

$$\frac{r}{t_c} = \frac{0.6}{0.25} = 2.44.$$

The scf are obtained from Figure A.7-1 of Bureau of Ship's Report PBL51-987 as follows:

$$K_B = 1.14$$

$$K_t = 1.28.$$

When these values are substituted into Equations (1), (2), and (3), the following stress values are obtained:

Outer surface of the cylinder

$$\frac{\sigma_t}{\sigma_{nom}} = 1.8$$

$$\frac{\sigma_n}{\sigma_{nom}} = 2.3$$

Inner surface of the sphere

$$\frac{\sigma_n}{\sigma_{nom}} = 2.6 .$$

## CONCLUSIONS

The principal sources of error in the calculated values of stress for the various models are the approximate influence coefficients used for the sphere, the relatively thick walls of the structures, the use of Poisson's ratio of 0.3 instead of 0.45 for the plastic models (see page 28 of Taylor et al.<sup>7</sup>) and the stress-concentration effect of the fillet.

The last effect mentioned is considered to be the most significant. This conclusion is based on the comparison of measured and calculated values in Figures 1 and 2. On these figures it is shown that when  $r/t_s \geq 0.5$  the agreement between the measured and calculated hoop and axial stresses is reasonably good for engineering purposes. Similarly, the agreement is reasonably good at the inside corner. Thus, the agreement between the calculated and measured values is fairly good for (1) those stresses which are little affected by the stress concentration effect of the outer fillet and (2) the condition when the fillet radius becomes large enough for the scf to approach unity. However, as the outer fillet radius is decreased, the difference between the calculated and measured axial stress approaches 100%.

A significant part of the difference between measured and calculated stresses for small values of  $r/t_s$  may be due to errors in the measured



stresses. This conclusion is supported by the test data as explained in the following discussion. Figures 1 and 2 show the same variation in the outer axial stress and the outer hoop stress with decreasing  $r/t_s$ . However, since the effect of the fillet would be expected to act directly on the axial stresses and only by a Poisson's ratio of the axial stress in the hoop direction, there should be a greater increase in the axial stress than occurs in the hoop stress as  $r/t_s$  decreases. That is, the measured axial stresses should show a sharper increase in gradient as  $r/t_s$  becomes smaller in the same manner as do the calculated stresses. This tendency of the axial stress to show no greater rate of change of stress than that shown by the hoop stress leads to the conclusion that the measured values of axial stress may be too low at low values of  $r/t_s$ .

In the foregoing discussion it is assumed that the material in the fillet is not sufficient to alter the discontinuity forces and moments. The assumption is supported by the fact that the stress at the inner corner is independent of the fillet radius. Thus, for the models used in Figures 1 and 2, the discontinuity forces and moments may be considered to be constant and the variation in stress to be due largely to the stress concentration effect of the fillet.

The results given in Table 1 are for models with the same fillet radius. For Models N-1A, N-1E, and N-3D, having a constant value of  $r/t_s = 0.555$ , the cylinder thickness was varied so that the variation in calculated stresses between the models was due to changing discontinuity forces and changing stress concentration factor. In these models, even though  $r/t_s$  was constant, the change in the cylinder wall thickness resulted in a change in the stress concentration values, since these were based on  $r/t_c$  values.

On the basis of the correlations with the test models, the following conclusions were reached:

1. Both the measurements and the calculations show that the size of the outside fillet radius has an important effect on the axial stress. The assumptions in the calculations used to obtain the discontinuity forces can have less effect on the final stress values than the stress concentration resulting from the size of the outer fillet radius. That is, the fillet can add more or less material where the axial force and moment are maximum without affecting their magnitude. At the same time, the fillet can change the geometrical contour which changes the stress concentration effect. Consequently, the axial stress can be made to vary widely with the choice of fillet radius without any change in the discontinuity forces and moments.
2. At small values of  $r/t_s$  the measured axial stresses may

be too low; hence the calculated values may not be as conservative as indicated by Figures 1 and 2.

3. Agreement between the calculated and the measured stresses indicates that reasonably good results can be expected from the calculations for a range of variables for

$$2.5 \leq R/a \leq 7.5,$$

$$0.268 \leq t_c/t_s \leq 1.0, \text{ and}$$

$$r/t_s \geq 0.5.$$

4. Test data in Figures 1 and 2 indicate that the inside corner radius has negligible effect on the stresses for  $0.1 \leq r/t_s \leq 0.7$ , where  $r$  is the inside corner radius.

#### REFERENCES

1. Timoshenko, S., Theory of Plates and Shells 1st ed. (New York: McGraw Hill Book Co., 1940).
2. Galletly, G. D., "Influence Coefficients for Hemispherical Shells with Small Openings at the Vertex," Journal of Applied Mechanics, Vol. 22, No. 1, March 1955, p. 20.
3. Peterson, R. E., Stress Concentration Design Factors (New York: John Wiley & Sons, Inc., 1953).
4. Heywood, R. B., Designing by Photoelasticity (London: Chapman and Hall Ltd., 1952).
5. Bureau of Ships, Department of the Navy, Tentative Structural Design Basis for Reactor Pressure Vessels and Directly Associated Components, PB 151-987 (Washington: Government Printing Office, 1958).
6. Taylor, C. E., Lind, N. C., and Schweiker, J. W., "A Three-Dimensional Photoelastic Study of Stresses Around Reinforced Outlets in Pressure Vessels," Paper No. 58-A-148 Contributed by the Power and Applied Mechanics Divisions at the Annual Meeting of ASME, New York, N. Y., November 30 - December 5, 1958.
7. Taylor, C. E., Lind, N. C., and Schweiker, J. W., "A Three-Dimensional Photoelastic Study of Stresses Around Reinforced Outlets in Pressure Vessels," Welding Research Council Bulletin Series No. 51, June 1959.
8. Taylor, C. E., Lind, N. C., and Cook, R. D., "Effect of Corner and Fillet Radii on Stress Concentrations in Spherical Shells with Cylindrical Outlets," TAM Report No. 581, University of Illinois, August 17, 1959.

APPENDIX I

DERIVATION OF DISCONTINUITY STRESSES AT THE JUNCTURE OF A CYLINDER AND SPHERE WITH A UNIFORM INTERNAL PRESSURE LOAD

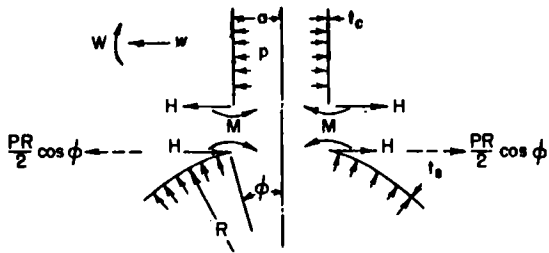


FIGURE A-1. ANALYTICAL MODEL WITH INTERNAL PRESSURE

Expressions for the rotation and deflection of the cylinder and the sphere are used to derive dimensionless formulas for the discontinuity bending and hoop stress on the outer surface (see Figure A.1), of the cylinder, at its juncture with the sphere, and in a latitude plane on the inside surface of the sphere. The slope and deflection of the cylinder must match that of the sphere at their junction. Then, we may set

$$w_c = w_s , \quad (1)$$

$$w_c = w_s ; \quad (2)$$

for the cylinder

$$w_c = \frac{H}{2\beta_c^3 D_c} - \frac{M_x}{\beta_c D_c} \quad (3)$$

and

$$w_c = \frac{H}{2\beta_c^3 D_c} - \frac{M_x}{2\beta_c^2 D_c} + \frac{pa^2}{Et_c} \left( 1 - \frac{\nu}{2} \right) , \quad (4)$$

and for the sphere

$$w_s = \frac{H}{2\beta_s^3 D_s} \sin \phi + \frac{M_x}{\beta_s D_s} - \frac{pR}{4\beta_s^3 D_s} \sin \phi \cos \phi \quad (5)$$

and

$$w_s = - \frac{H}{2\beta_s^3 D_s} \sin^2 \phi - \frac{M_x}{2\beta_s^2 D_s} \sin \phi + \frac{pR}{4\beta_s^3 D_s} \sin^2 \phi \cos \phi + \frac{pR^2}{2Et_s} (1 - \nu) \sin \phi , \quad (6)$$

A.2

where

$$\beta_c = \sqrt[4]{\frac{3(1 - \nu^2)}{a^2 t_c^2}} \quad (7)$$

$$\beta_s = \sqrt[4]{\frac{3(1 - \nu^2)}{R^2 t_s^2}} \quad (8)$$

$$D_c = \frac{Et_c^3}{12(1 - \nu^2)} \quad (9)$$

$$D_s = \frac{Et_s^3}{12(1 - \nu^2)} \quad (10)$$

$$\sin \phi = \frac{a}{R} \quad (11)$$

$$\cos \phi = \sqrt{1 - \left(\frac{a}{R}\right)^2} \quad (12)$$

The bending stress on the outer surface of the cylinder is given by

$$\sigma_{bc} = \frac{6M_x}{t_c^2} \quad (13)$$

The hoop stress on the outer surface of the cylinder due to the discontinuity effect only is given by

$$\begin{aligned} \sigma_{yc} &= \frac{w_{c1}}{a} E + \nu \sigma_{bc} \\ &= \frac{E}{a} \left\{ \frac{1}{2\beta_c^2 D_c} \left[ \frac{H}{\beta_c} - M_x \right] \right\} + \nu \sigma_{bc} \quad (14) \end{aligned}$$

Equations (3) through (12) are used to solve for  $M_x$  and  $H$  from Equations (1) and (2). The nondimensional bending stress in the cylinder is given by

$$\frac{\sigma_{bc}}{\sigma_{nom}} = \frac{\left[1 - \left(\frac{t_c}{t_s}\right)^2\right]}{2 \left[1 + \sqrt{\frac{R}{a}} \left(\frac{t_c}{t_s}\right)^{5/2}\right] \left[1 + \frac{1}{\sqrt{\frac{R}{a}}} \left(\frac{t_c}{t_s}\right)^{3/2}\right] - \left[1 - \left(\frac{t_c}{t_s}\right)^2\right]^2} \left\{0.634 \left(\frac{R}{a}\right) \left(\frac{t_c}{t_s}\right) - 1.54\right\}$$

$$+ \frac{2.33 \sqrt{\frac{R}{t_s}} \left\{ \sqrt{\frac{R}{a}} \left(\frac{t_c}{t_s}\right)^{3/2} \left[1 + \frac{1}{\sqrt{\frac{R}{a}}} \left(\frac{t_c}{t_s}\right)^{3/2}\right] + \frac{t_c}{t_s} \left[1 - \left(\frac{t_c}{t_s}\right)^2\right] \right\} \sqrt{1 - \left(\frac{1}{\frac{R}{a}}\right)^2}}{2 \left[1 + \sqrt{\frac{R}{a}} \left(\frac{t_c}{t_s}\right)^{5/2}\right] \left[1 + \frac{1}{\sqrt{\frac{R}{a}}} \left(\frac{t_c}{t_s}\right)^{3/2}\right] - \left[1 - \left(\frac{t_c}{t_s}\right)^2\right]^2}$$

where  $\sigma_{nom} = \frac{pa}{t_c}$  is the hoop-membrane stress in the cylinder. (16)

The nondimensional hoop stress due to discontinuity effects on the outer surface of the cylinder is given by:

$$\frac{\sigma_{yc}}{\sigma_{nom}} = \frac{1.104 \left[1 + \sqrt{\frac{R}{a}} \left(\frac{t_c}{t_s}\right)^{5/2}\right] - 0.252 \left[1 - \left(\frac{t_c}{t_s}\right)^2\right]}{2 \left[1 + \sqrt{\frac{R}{a}} \left(\frac{t_c}{t_s}\right)^{5/2}\right] \left[1 + \frac{1}{\sqrt{\frac{R}{a}}} \left(\frac{t_c}{t_s}\right)^{3/2}\right] - \left[1 - \left(\frac{t_c}{t_s}\right)^2\right]^2} \left\{0.634 \left(\frac{R}{a}\right) \left(\frac{t_c}{t_s}\right) - 1.54\right\}$$

$$+ 2.33 \sqrt{\frac{R}{t_s}} \left\{ \frac{\left[ \sqrt{\frac{R}{a}} \left(\frac{t_c}{t_s}\right)^{3/2} \left[1 + \frac{1}{\sqrt{\frac{R}{a}}} \left(\frac{t_c}{t_s}\right)^{3/2}\right] + \frac{t_c}{t_s} \left[1 - \left(\frac{t_c}{t_s}\right)^2\right] \right]}{2 \left[1 + \sqrt{\frac{R}{a}} \left(\frac{t_c}{t_s}\right)^{5/2}\right] \left[1 + \frac{1}{\sqrt{\frac{R}{a}}} \left(\frac{t_c}{t_s}\right)^{3/2}\right] - \left[1 - \left(\frac{t_c}{t_s}\right)^2\right]^2} \right.$$

$$\left. \left[ \frac{1.104 \left[1 + \sqrt{\frac{R}{a}} \left(\frac{t_c}{t_s}\right)^{5/2}\right]}{\left[1 - \left(\frac{t_c}{t_s}\right)^2\right]} - 0.252 \right] - \frac{0.552 \left(\frac{t_c}{t_s}\right)^{3/2} \sqrt{\frac{R}{a}}}{\left[1 - \left(\frac{t_c}{t_s}\right)^2\right]} \right\} \sqrt{1 - \left(\frac{1}{\frac{R}{a}}\right)^2}$$

The bending stress on the inside surface of the sphere due to the discontinuity effects is given by

$$\sigma_{bs} = \frac{6M_x}{t_s^2} \quad (18)$$

A.4

or

$$\sigma_{b_s} = \left(\frac{t_c}{t_s}\right)^2 \sigma_{b_c} \quad (19)$$

In the latitude plane of the opening the hoop stress on the inside surface of the sphere which is caused by the discontinuity effects is given by:

$$\sigma_{y_s} = \frac{w_{s1}}{a} E - \nu \sigma_{b_s}$$

or

$$= \left[ \frac{pR}{4\beta_s^3 D_s} \sin^2 \phi \cos \phi - \frac{M}{2\beta_s^2 D_s} \sin \phi - \frac{H}{2\beta_s^3 D_s} \sin^2 \phi \right] \frac{E}{a} - \nu \sigma_{b_s} \quad (20)$$

The nondimensional hoop stress in the sphere is given by:

$$\frac{\sigma_{y_s}}{\sigma_{nom}} = \frac{-1.104 \sqrt{\frac{t_c}{t_s}}}{\left(\frac{R}{a}\right)^{3/2}} \left\{ \frac{1.136 \sqrt{\frac{t_c}{t_s}} \sqrt{\frac{R}{a}} \left[ 1 - \left(\frac{t_c}{t_s}\right)^2 \right] + 2 \left[ 1 + \sqrt{\frac{R}{a}} \left(\frac{t_c}{t_s}\right)^{5/2} \right]}{2 \left[ 1 + \sqrt{\frac{R}{a}} \left(\frac{t_c}{t_s}\right)^{5/2} \right] \left[ 1 + \frac{1}{\sqrt{\frac{R}{a}}} \left(\frac{t_c}{t_s}\right)^{5/2} \right] - \left[ 1 - \left(\frac{t_c}{t_s}\right)^2 \right]^2} \right. \\ \left. \left\{ 0.634 \left(\frac{R}{a}\right) \left(\frac{t_c}{t_s}\right) - 1.54 \right\} + 2.33 \sqrt{\frac{R}{t_s}} \left[ \frac{1.104}{\frac{R}{a} \left[ 1 - \left(\frac{t_c}{t_s}\right)^2 \right]} \right] \right. \\ \left. - \frac{1.104 \sqrt{\frac{t_c}{t_s}}}{\left(\frac{R}{a}\right)^{3/2} \left[ 1 - \left(\frac{t_c}{t_s}\right)^2 \right]} \left\{ 1.136 \sqrt{\frac{t_c}{t_s}} \sqrt{\frac{R}{a}} \left[ 1 - \left(\frac{t_c}{t_s}\right)^2 \right] + 2 \left[ 1 + \sqrt{\frac{R}{a}} \left(\frac{t_c}{t_s}\right)^{5/2} \right] \right\} \right. \\ \left. \left[ \frac{\sqrt{\frac{R}{a}} \left(\frac{t_c}{t_s}\right)^{3/2} \left[ 1 + \frac{1}{\sqrt{\frac{R}{a}}} \left(\frac{t_c}{t_s}\right)^{3/2} \right] + \frac{t_c}{t_s} \left[ 1 - \left(\frac{t_c}{t_s}\right)^2 \right]}{2 \left[ 1 + \sqrt{\frac{R}{a}} \left(\frac{t_c}{t_s}\right)^{5/2} \right] \left[ 1 + \frac{1}{\sqrt{\frac{R}{a}}} \left(\frac{t_c}{t_s}\right)^{3/2} \right] - \left[ 1 - \left(\frac{t_c}{t_s}\right)^2 \right]^2} \right] \right\} \sqrt{1 - \left(\frac{1}{\frac{R}{a}}\right)^2} \quad (21)$$

where  $\sigma_{nom} = \frac{pR}{2t_s}$  is the membrane stress in the sphere. (22)

## APPENDIX II

DERIVATION OF DISCONTINUITY STRESSES AT THE JUNCTURE OF A CYLINDER AND  
 SPHERE WITH A DIFFERENCE IN AVERAGE WALL TEMPERATURE  
 BETWEEN THE CYLINDER AND SPHERE

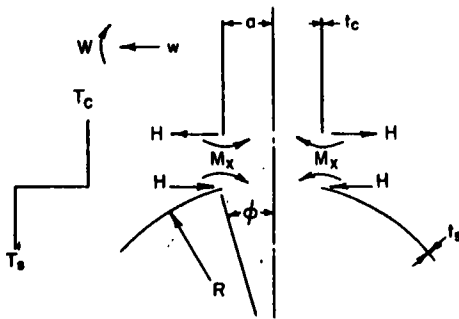


FIGURE A-2. ANALYTICAL MODEL WITH  
 "STEP" TEMPERATURE CHARGE

When the differential temperature loading is considered, the equations for the slope and displacement of the cylinder and sphere at their juncture are (see Figure A.2):

$$w_c = \frac{H}{2\beta_c^2 D_c} - \frac{M_x}{\beta_c D_c} \quad (23)$$

$$w_c = \frac{H}{2\beta_s^2 D_s} - \frac{M_x}{2\beta_c^2 D_c} + a\alpha T_c \quad (24)$$

$$w_s = \frac{H}{2\beta_s^2 D_s} \sin \phi + \frac{M_x}{\beta_s D_s} \quad (25)$$

$$w_s = -\frac{H}{2\beta_s^2 D_s} \sin^2 \phi - \frac{M_x}{2\beta_s^2 D_s} \sin \phi + a\alpha T_s \quad (26)$$

We may solve for  $H$  and  $M_x$  with Equations (1) and (2). Knowing  $H$  and  $M_x$ , the bending stress in the cylinder, we may obtain the hoop stress in the cylinder and the hoop stress in the sphere from Equations (13), (14), and (20).

The nondimensional stresses caused by the difference in temperature between the cylinder and sphere are as follows. The bending stress in the cylinder is

$$\frac{\sigma_{bc}}{E\alpha\Delta T} = \frac{1.82 \left[ 1 - \left( \frac{t_c}{t_s} \right)^2 \right]}{2 \left[ 1 + \sqrt{\frac{R}{a}} \left( \frac{t_c}{t_s} \right)^{5/2} \right] \left[ 1 + \frac{1}{\sqrt{\frac{R}{a}}} \left( \frac{t_c}{t_s} \right)^{3/2} \right] - \left[ 1 - \left( \frac{t_c}{t_s} \right)^2 \right]^2}, \quad (27)$$

where

$$\Delta T = (T_s - T_c) \quad (28)$$

The hoop stress on the outer surface of the cylinder is given by

$$\frac{\sigma_n}{E\alpha\Delta T} = \frac{2 \left[ 1 + \sqrt{\frac{R}{a}} \left( \frac{t_c}{t_s} \right)^{5/2} \right] - 0.456 \left[ 1 - \left( \frac{t_c}{t_s} \right)^2 \right]}{2 \left[ 1 + \sqrt{\frac{R}{a}} \left( \frac{t_c}{t_s} \right)^{5/2} \right] \left[ 1 + \frac{1}{\sqrt{\frac{R}{a}}} \left( \frac{t_c}{t_s} \right)^{3/2} \right] - \left[ 1 - \left( \frac{t_c}{t_s} \right)^2 \right]^2} \quad (29)$$

The hoop stress in the latitude plane of the opening on the inside of the sphere is given by

$$\frac{\sigma_n}{E\alpha\Delta T} = - \frac{\left( \frac{t_c}{t_s} \right)^{3/2} \left\{ 2 \left[ 1 + \sqrt{\frac{R}{a}} \left( \frac{t_c}{t_s} \right)^{5/2} \right] + 1.545 \sqrt{\frac{R}{a}} \sqrt{\frac{t_c}{t_s}} \left[ 1 - \left( \frac{t_c}{t_s} \right)^2 \right] \right\}}{\sqrt{\frac{R}{a}} \left\{ 2 \left[ 1 + \sqrt{\frac{R}{a}} \left( \frac{t_c}{t_s} \right)^{5/2} \right] \left[ 1 + \frac{1}{\sqrt{\frac{R}{a}}} \left( \frac{t_c}{t_s} \right)^{3/2} \right] - \left[ 1 - \left( \frac{t_c}{t_s} \right)^2 \right]^2 \right\}} \quad (30)$$

The influence coefficients relating the edge forces and moments to the edge rotations and deflections for the cylinder and sphere are derived in the "Theory of Plates and Shells" by S. Timoshenko.<sup>1</sup> The influence coefficients for the sphere are based on an approximate analysis in which the portion of the sphere near the edge is replaced by a tangent conical shell; the equation developed for the circular cylinder is used to obtain a solution for this conical shell.

The influence coefficients used for the edge moment and shear force are obtained from Timoshenko's<sup>2</sup> equations by substituting  $\lambda = \beta_{sa}$ .

<sup>1</sup>Timoshenko, S., Theory of Plates and Shells, 1st ed. (New York: McGraw Hill Book Co., 1940).

<sup>2</sup>ibid pages 470-471.



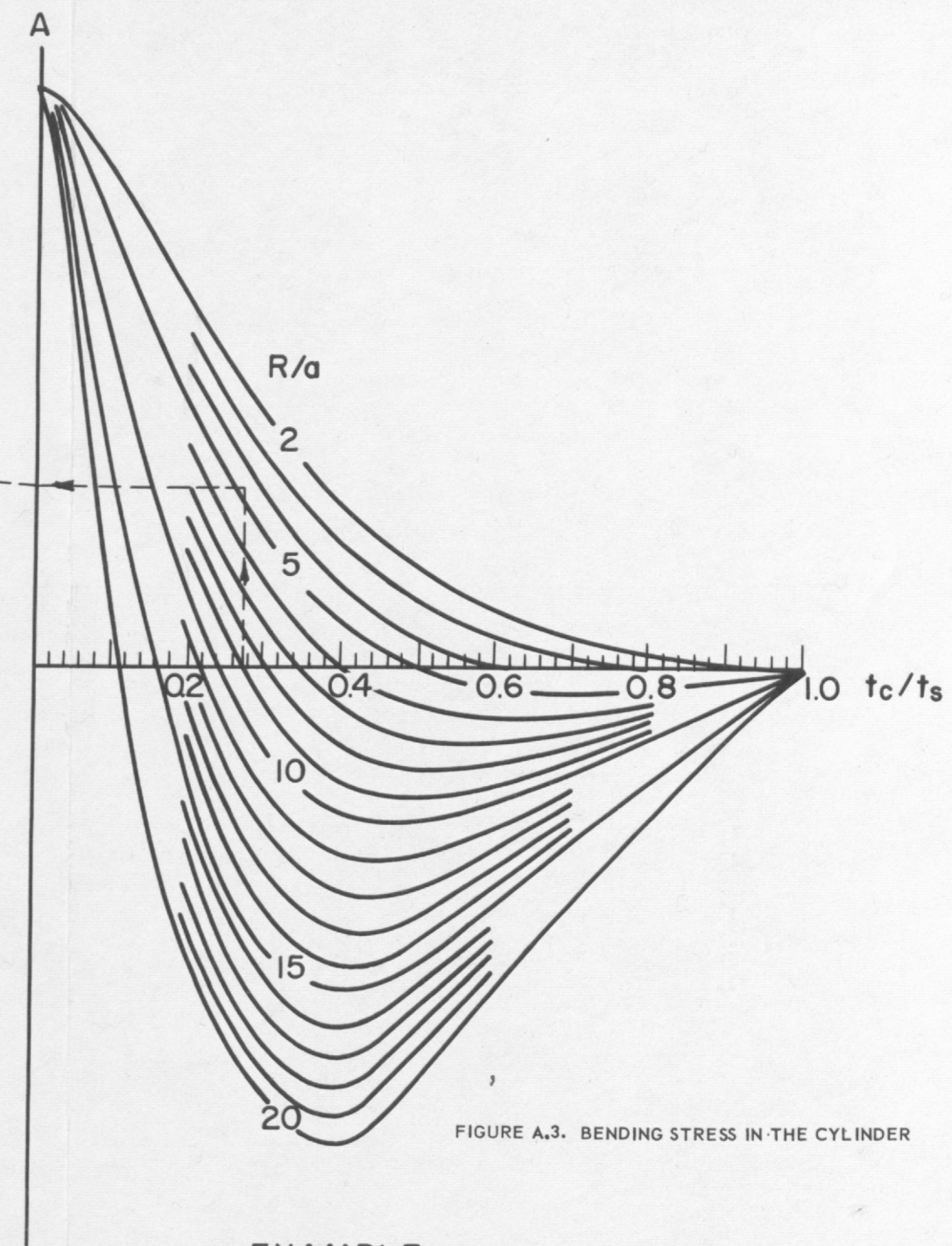
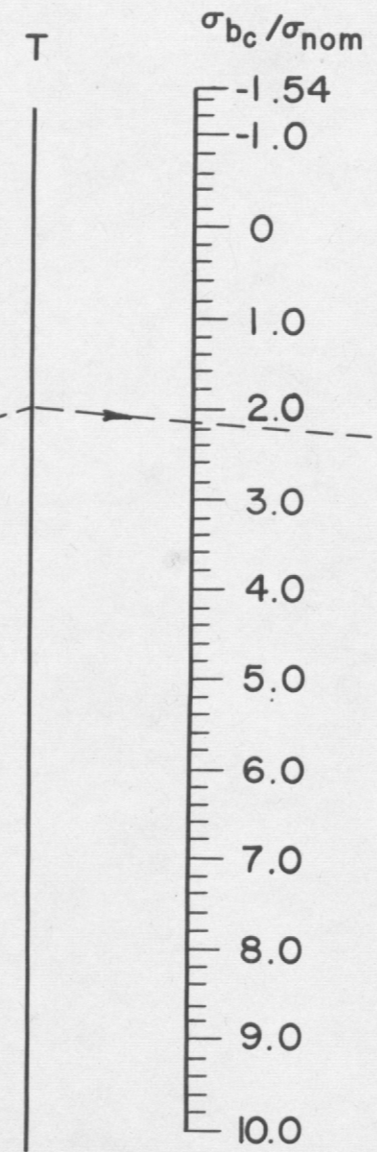
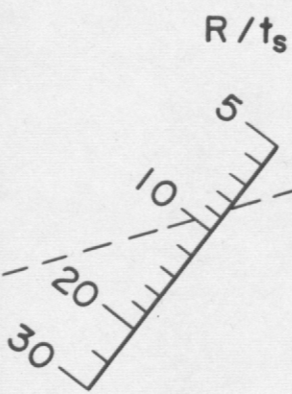
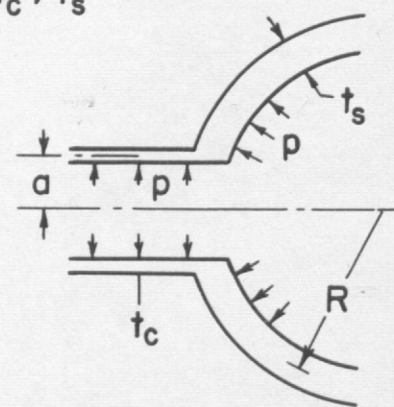
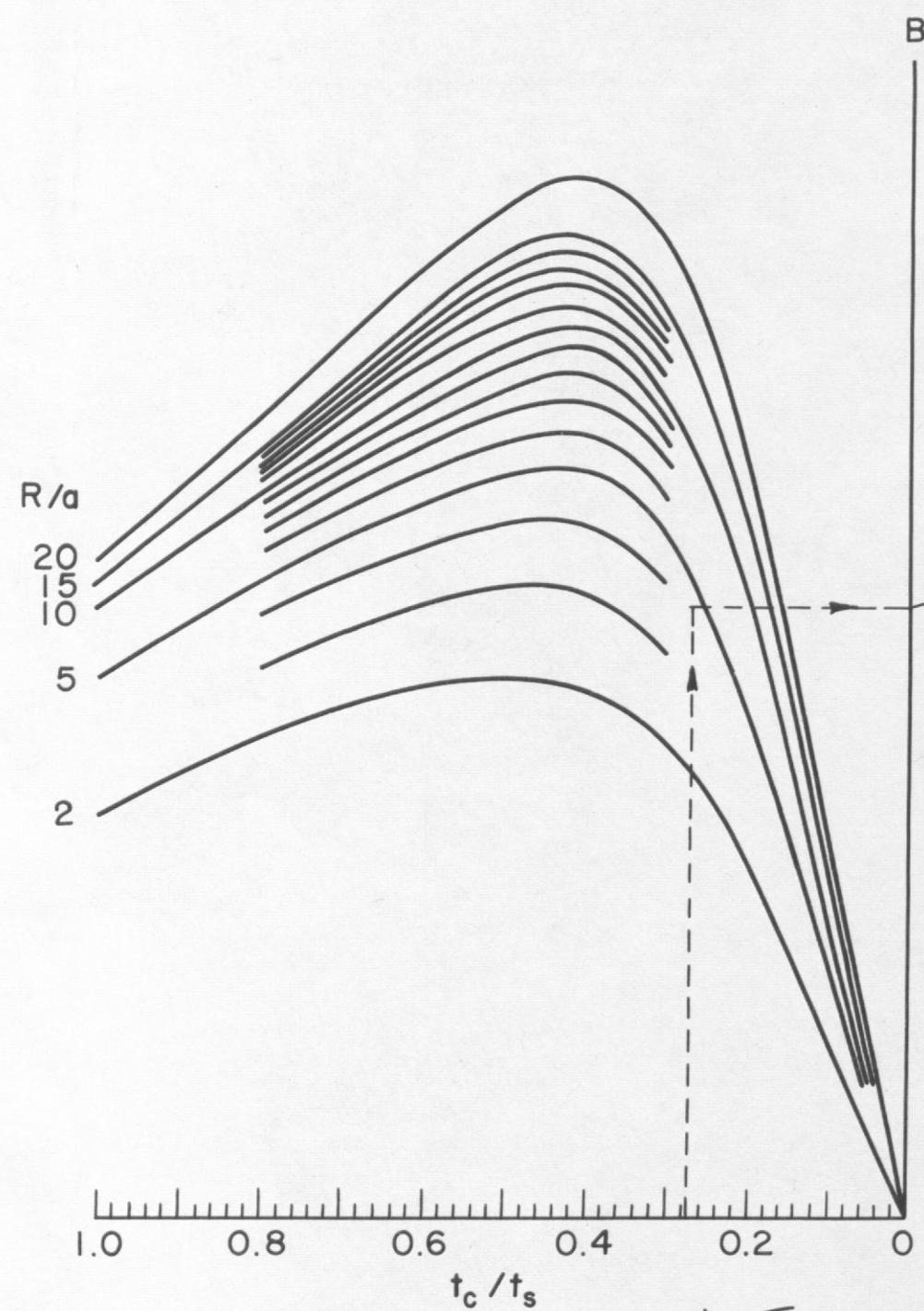


FIGURE A.3. BENDING STRESS IN THE CYLINDER

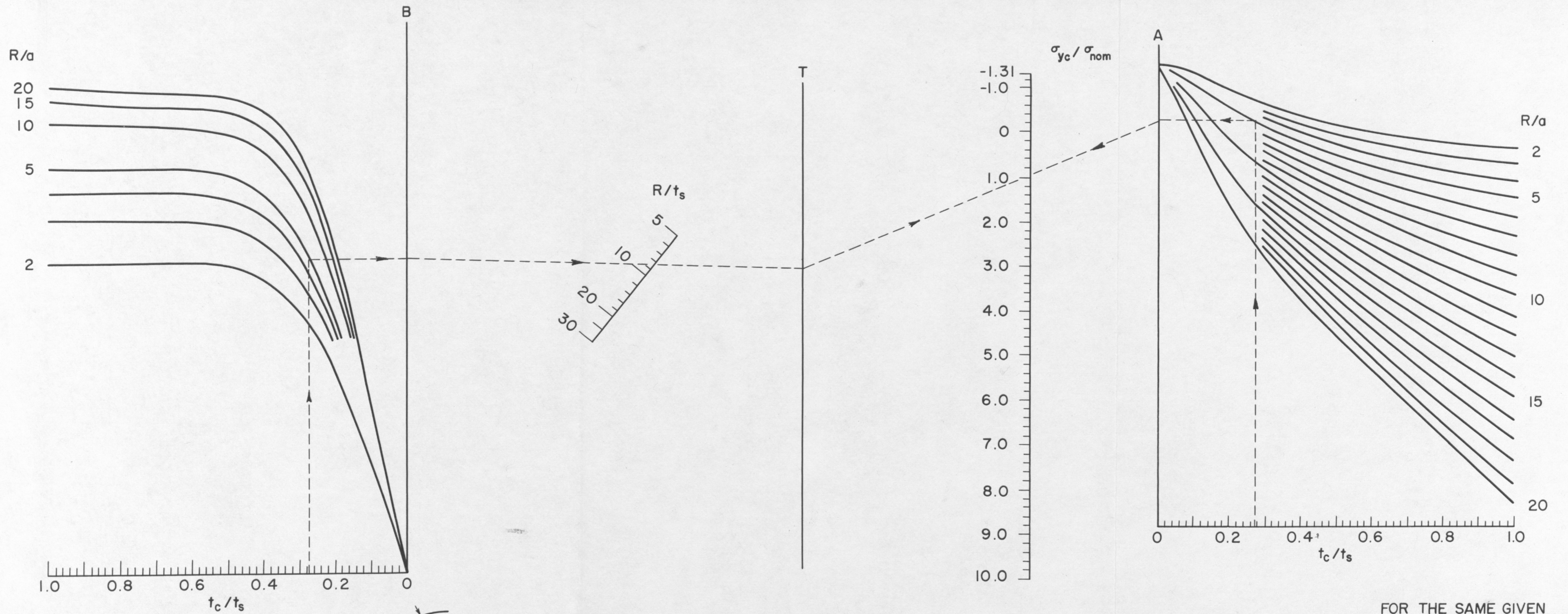
**EXAMPLE**

GIVEN:  $t_c/t_s = 0.278$   $R/a = 4.77$ ,  $R/t_s = 8.28$   
 FIND:  $\sigma_{b_c}/\sigma_{nom}$

**SOLUTION:**

- (1) LOCATE POINT ON "B" FOR  $t_c/t_s = 0.278$  AND  $R/a = 5$
- (2) CONNECT POINT ON "B" WITH  $R/t_s = 8.28$  TO LOCATE A POINT ON "T"
- (3) LOCATE POINT ON "A" FOR  $t_c/t_s = 0.278$  AND  $R/a = 4.77$
- (4) CONNECT POINT ON "A" WITH POINT ON "T" AND READ  
 $\sigma_b/\sigma_{nom} = 2.1$   $\sigma_{nom} = \frac{pa}{t_c}$





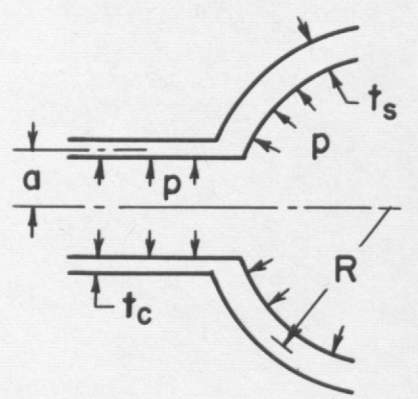
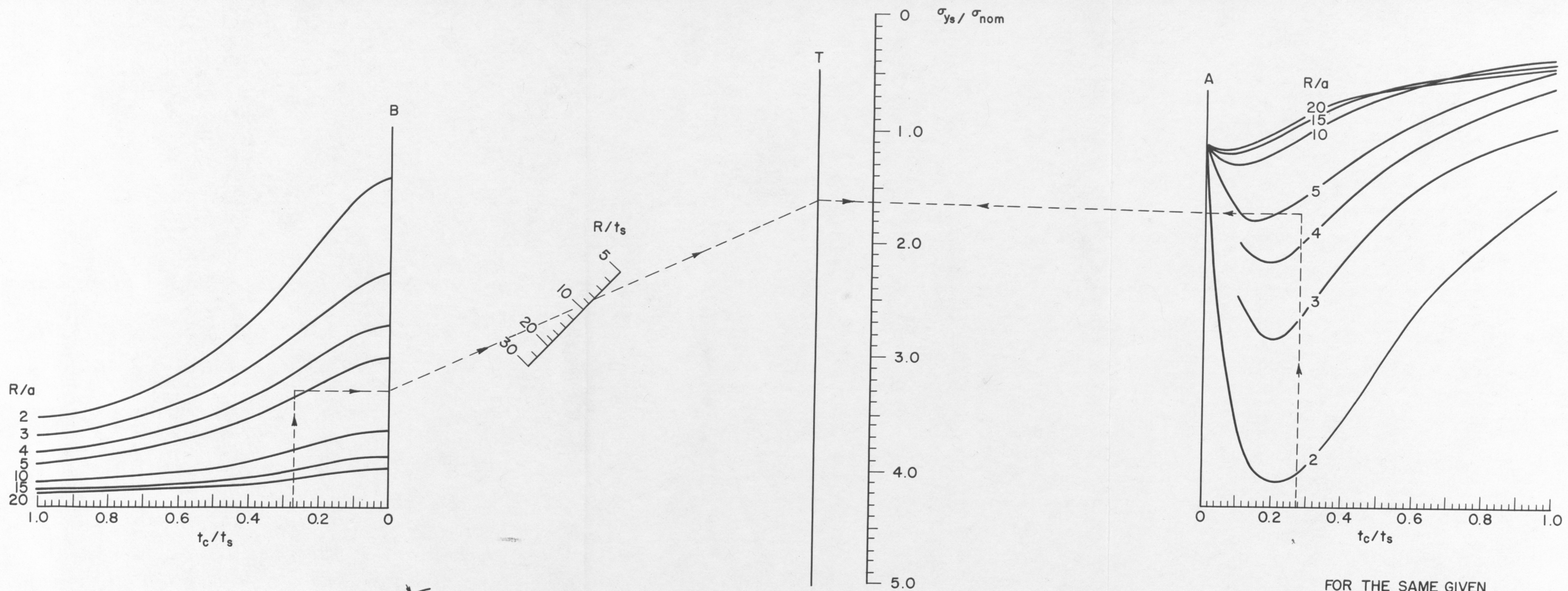
FOR THE SAME GIVEN PARAMETERS THE HOOP STRESS IN THE CYLINDER IS OBTAINED IN THE SAME MANNER AS THE BENDING STRESS.

$$\frac{\sigma_{yc}}{\sigma_{nom}} = 1.0$$

$$\sigma_{nom} = \frac{pa}{t_c}$$

FIGURE A.4. HOOP STRESS IN THE CYLINDER





FOR THE SAME GIVEN PARAMETERS THE HOOP STRESS IN THE SPHERE IS OBTAINED IN THE SAME MANNER AS THE BENDING STRESS IN THE CYLINDER.

$$\frac{\sigma_{ys}}{\sigma_{nom}} = 1.6$$

$$\sigma_{nom} = \frac{pR}{2t_s}$$

FIGURE A.5. HOOP STRESS IN THE SPHERE





